

The Swelling-Activated Anion Conductance in the Mouse Renal Inner Medullary Collecting Duct Cell Line mIMCD-K2

S.H. Boese, M. Glanville, M.A. Gray, N.L. Simmons

Department of Physiological Sciences, Medical School, Framlington Place, University of Newcastle upon Tyne, Newcastle upon Tyne, NE2 4HH, UK

Received: 24 February 2000/Revised: 26 May 2000

Abstract. Swelling-activated Cl^- currents ($I_{\text{Cl,swell}}$) have been characterized in a mouse renal inner medullary collecting duct cell line (mIMCD-K2). Currents activated by exposing the cells to hypotonicity exhibited characteristic outward rectification and time- and voltage-dependent inactivation at positive potentials and showed an anion selectivity of $\text{I}^- > \text{Br}^- > \text{Cl}^- > \text{Asp}^-$. NPPB (100 μM) inhibited the current in a voltage independent manner, as did exposure to 10 μM tamoxifen and 500 μM niflumic acid (NFA). In contrast, DIDS (100 μM) blocked the current with a characteristic voltage dependency. These characteristics of $I_{\text{Cl,swell}}$ in mIMCD-K2 cells are essentially identical to those of heterologously expressed cardiac CLC-3.

A defining feature of CLC-3 is that activation of PKC by PDBu inhibits the conductance. In mIMCD-K2 cells preincubation with PDBu (100 nM) prevented the activation of $I_{\text{Cl,swell}}$ by hypotonicity. However, PDBu inhibition of $I_{\text{Cl,swell}}$ was reversed after PDBu withdrawal, but this was refractory to subsequent PDBu inhibition. Activation of either the cystic fibrosis transmembrane conductance regulator (CFTR) or Ca^{2+} activated Cl^- conductance (CaCC), which are coexpressed in mIMCD-K2 cells prior to PDBu treatment, abolished the PDBu inhibition of $I_{\text{Cl,swell}}$. Control of $I_{\text{Cl,swell}}$ by PKC therefore depends on the physiological status of the cell.

In intact mIMCD-K2 layers in Ussing chambers, forskolin stimulation of an inward short-circuit current (due to transepithelial Cl^- secretion via apical CFTR) was inhibited by cell swelling upon hypotonic exposure at the basolateral surface. Activation of $I_{\text{Cl,swell}}$ is therefore capable of regulating transepithelial Cl^- secretion and suggests that $I_{\text{Cl,swell}}$ is located at the basolateral

membrane. PDBu exposure prior to or during hypotonic challenge was ineffective in reversing the swelling-activated inhibition of Cl^- secretion, but tamoxifen (100 μM) abolished the hypotonic inhibition of forskolin-stimulated short-circuit current (I_{sc}).

RT-PCR analysis confirmed expression of mRNA for members of the CLC family, including both CLC-2 and 3, in the mIMCD-K2 cell line.

Key words: $I_{\text{Cl,swell}}$ — mIMCD-K2 — PKC — CLC conductance

Introduction

Cells of the renal medullary-collecting duct are normally exposed to large variations in external osmolarity [2]. To cope with these changes the cell can activate a variety of transport proteins in the plasma membrane (for review see [20]).

Swelling-activated anion/organic osmolyte channels play a major part in cell volume recovery after hypoosmotic perturbation in the renal inner medullary collecting ducts (IMCD) (see [23] for review). Though the biophysical and pharmacological properties of these channels have been well characterized in rat IMCD cells in primary cell culture [7, 8, 33], the cellular location and molecular identity of this conductance remains uncertain.

Several proteins have been proposed to be the molecular entity responsible for $I_{\text{Cl,swell}}$ (for reviews see [29, 34]), including P-glycoprotein (P-gp) [37] and the pI_{Cln} protein [30]. However, recent work indicates that neither is a Cl^- channel [12]. Instead, P-gp may play a regulatory role in cell volume regulation [38], overexpression of P-gp possibly altering cytoskeleton/membrane interactions, which then in turn modify the activity of volume-sensitive Cl^- channels [34]. pI_{Cln} is now

known to reside in the cytoplasm [15] and may be best regarded as being responsible for regulating the structure and function of the cytoskeleton, and/or a protein involved in mediating interactions between components of intracellular signal transduction pathways [16]. Experimental perturbation of pI_{Cln} alters the architecture of the cytoskeleton, which has an influence on $I_{Cl,swell}$ (see [35]).

Members of the CLC voltage-gated Cl^- channel family have also been implicated in cell volume regulation. CLC-2 was shown to be activated by cell swelling after expression in *Xenopus* oocytes [18] and Sf-9 insect cells [43]. The characteristics of CLC-2 currents are, however, substantially different from $I_{Cl,swell}$. In addition, Bond et al. [9] showed that in T84 cells both $I_{Cl,swell}$ and CLC-2 type Cl^- conductances are present, but only the former appeared to be relevant to RVD (Regulatory Volume Decrease).

The most recent protein considered to be responsible for $I_{Cl,swell}$ is CLC-3 (see [39] for review). CLC-3 was first characterized by Kawasaki et al. in 1994 [22] and is ubiquitously expressed, but with high expression levels in kidney, lung and brain. Heterologous expression of CLC-3 in *Xenopus* oocytes produced a large time-independent, slightly outwardly rectifying Cl^- current. The anion selectivity was $\text{I}^- > \text{Br}^- = \text{Cl}^- > \text{acetate} > \text{gluconate}$. DIDS as well as the PKC activators TPA and PDBu inhibited the conductance. Duan et al. [13] showed that functional expression of a cardiac clone of CLC-3 from guinea pig in NIH/3T3 cells resulted in a swelling-activated anion conductance with similar characteristics. The conductance showed outward rectification but with time- and voltage-dependent inactivation at high positive potentials, an anion selectivity of $\text{I}^- > \text{Cl}^-$ and inhibition by DIDS, tamoxifen, extracellular ATP, and by the PKC activator PDBu. Furthermore, Duan et al. [14] were able to link PKC modulation of $I_{Cl,swell}$ with CLC-3 protein phosphorylation.

The biophysical and pharmacological characteristics of CLC-3 shown by Duan et al. [13] are virtually identical to $I_{Cl,swell}$ in brain endothelial cells [42]. Since RT-PCR analysis showed high level expression of CLC-3 mRNA, they proposed that CLC-3 is likely to be the channel that mediates $I_{Cl,swell}$ or at least participates in the RVD response in brain endothelial cells. In addition, Yamazaki et al. [44] have demonstrated a swelling-activated anion current with similar functional characteristics to CLC-3 in canine vascular smooth muscle cells in combination with a high level of CLC-3 mRNA expression.

Both CLC-2 and CLC-3 are expressed in the kidney (e.g. [28]), with subpopulations of epithelial cells along the nephron showing distinct patterns of expression. To overcome the inherent limitations of isolated nephron segments and cells in primary cell culture we have

chosen a homogeneous established murine cell-line, mIMCD-K2, to characterize the swelling-activated anion conductance. This cell-line was established from the initial segment of the terminal IMCD and we have shown that these cells coexpress the CFTR Cl^- conductance as well as a Ca^{2+} -activated Cl^- conductance [4]. Using functional criteria we have attempted to localize $I_{Cl,swell}$ in polarized epithelial cells and have determined whether $I_{Cl,swell}$ may be linked to CLC-3 expression by use of a combination of molecular methods (RT-PCR) and functional criteria (e.g., PDBu inhibition). (Parts of these data have been published in abstract form [5, 6].)

Material and Methods

CELL CULTURE

mIMCD-K2 cells [24] were kindly provided by Dr. Bruce Stanton (Dartmouth Medical School, Hanover, New Hampshire). mIMCD-K2 cells (18–25 passages) were routinely cultured in Opti-MEM medium supplemented with 5 mM l-glutamine, 50 $\mu\text{g}/\text{ml}$ penicillin/streptomycin and 10% v/v fetal bovine serum at 37°C in an air/5% CO_2 atmosphere. Stock Roux bottles (75 cm^2 growth area) were coated with Vitrage/Cellon collagen and cells were passaged by trypsinization (2 ml of 0.5% w/v trypsin, 0.7 mM EDTA in $\text{Ca}^{2+}/\text{Mg}^{2+}$ free saline) to form a cell suspension and culturing at a 1:10 split ratio. Functional epithelial layers of mIMCD-K2 cells were prepared by high-density seeding ($2 \times 10^5 \text{ cells}/\text{cm}^2$) on to Vitrage/Cellon-coated permeable filter supports (Snapwell, Costar, 12 mm diameter, 0.4 μm pore diameter). Filter supports were then cultured in 6-well plates at 37°C (air/5% CO_2) for up to 14 days with medium replacement every 2–3 days. For patch-clamp recording and for intracellular Ca^{2+} measurements cells were seeded at low density (1.7×10^4 cells) onto coverslips (24 mm diameter) and cultured as for filter supported layers.

MEASUREMENTS OF SHORT-CIRCUIT CURRENT AND EPITHELIAL RESISTANCE

Cultured epithelial layers were mounted in Ussing type chambers maintained at 37°C, connected to an automatic voltage clamp (WPI Instruments, DVC-1000, New Haven, CT) via KCl/agar salt-bridges and reversible electrodes (Ag/AgCl for current passage, calomel for voltage sensing). Measurements of open-circuit electrical potential difference (p.d.), transepithelial resistance (R_t) and short-circuit current (I_{sc}) were made in modified Krebs solutions (see below).

WHOLE-CELL PATCH-CLAMP ANALYSIS

mIMCD-K2 cells grown on coverslips were continuously superfused at 5 ml/min (volume of tubing switch ~1 ml, chamber volume ~0.5 ml) at room temperature while membrane currents were measured using the nystatin slow whole-cell configuration of the patch-clamp technique and in some experiments the fast whole-cell configuration [19]. Patch pipettes were made from borosilicate glass and had resistances, after fire polishing, of 3 to 5 $\text{M}\Omega$. Seal resistance was typically between 5 and 20 $\text{G}\Omega$.

Whole-cell currents were measured with an EPC9 patch-clamp amplifier (HEKA Electronics, Lambrecht, Germany) at a holding potential of 0 or -60 mV with excursions from -80/-100 mV to +80/120

mV in 20 mV increments. Voltage stimulation and data acquisition were achieved using 16-bit DA and AD converters (ITC-16, Instrutech, Washington Port, New York), controlled by a PC, using the Pulse software (HEKA Electronics). Data were filtered at 1 or 0.5 kHz and sampled at 2 kHz and stored on the computer hard disk. Data were analyzed using PulseFit and PulseTools (HEKA Electronics). Junction potentials were corrected, and cell capacitance and series resistance was compensated. The slope conductance was obtained by linear regression of the current at the reversal potential. Reversal potentials were determined from 1 sec-voltage ramps (-80 to +80 mV).

In basal conditions with the standard bath and pipette solutions the measured cell capacitance (EPC9 compensation circuit) was 23.4 ± 2.6 pF ($n = 99$).

Determination of expression of CLC-2/3 mRNA transcripts by Reverse Transcription-Polymerase Chain Reaction (RT-PCR).

RNA Extraction from mIMCD-K2

Confluent cell layers were briefly washed (3 times) with phosphate buffered saline (2.7 mM KCl, 1.47 mM KH_2PO_4 , 137 mM NaCl, 8 mM $\text{Na}_2\text{HPO}_4 \cdot 7\text{H}_2\text{O}$). A 10-min incubation in lysis buffer (5 ml, 200 mM NaCl, 200 mM tris-HCl, pH 7.5, 1.5 mM MgCl₂, 4.7 mM disodium EDTA, 2% SDS, 1 μg proteinase K) at 20°C. Cell disruption was completed by titration through a 21-gauge needle, followed by incubation at 45°C for 1 hr. Sodium chloride was added to a final concentration of 500 mM before repeated resuspension, as above.

mRNA was purified from total RNA in lysis buffer (cells or tissue) by the use of an oligo-dT resin method (Pharmacia Biotech, St. Albans, Herts, UK). Poly-A⁺ RNA, eluted from the oligo-dT, was precipitated by the addition of 40 μl of 3M $\text{C}_2\text{H}_3\text{O}_2\text{Na}$ (pH 5.2) and 1 ml of 100% ethanol. After centrifugation (30,000 $\times g$ for 1 hr at 4°C) the solution was decanted and the pellet air-dried for 5 min before adding 100 μl of Tris-HCl, pH 8.5. This was incubated at 65°C for 10 min to aid dissolution. Quantification of purity and yield of mRNA was made by UV absorption at 260 nm and 280 nm.

Reverse Transcription (RT)

Poly-A⁺ RNA (1 μg) was reverse transcribed in a buffer (50 mM Tris-HCl pH 8.3, 50 mM KCl, 4 mM MgCl₂, 10 mM DTT), containing 0.5 mM dNTPs (MBI Fermentas, Sunderland, UK), 10 units Moloney murine leukemia virus reverse transcriptase (M-MuLV RT MBI Fermentas), 20 units RNase inhibitor (MBI Fermentas) and 0.023 units random hexamer primers (Pharmacia Biotech) at 42°C for 1 hr. Omission of M-MuLV RT provided a negative control for DNA contamination.

Polymerase Chain Reaction (PCR)

PCR reactions were performed in a buffer (10 mM tris-HCl, pH 8.8, 50 mM NaCl, 2 mM MgCl₂, 0.08% Nonidet P40), containing 0.2 mM dNTPs, 1.25 units recombinant Taq DNA polymerase (MBI Fermentas) and 0.5 μM forward and reverse primers using the PCR Express Thermal Cycler (Hybaid, Teddington, Middlesex, UK) for 30 amplification cycles. Each cycle consisted of 94°C for 30 sec, 54°C and 55°C for 30 sec and 72°C for 60 sec.

Oligonucleotide primers for CLC-2/3 were designed from rat (CLC-2, Accession No. X64139) and mouse (CLC-3, Accession No. AF029347) sequences using Primer3 software (www.genome.wi.mit.edu/cgi-bin/primer/primer3.cgi). Forward primers 5'-TCTCAGC-AAGTTCTCTCC-3' and 5'-TCTTCCAAAGTATAGCACC-3', reverse primers 5'-GCCACTAGCAATACCAATGAC-3' and 5'-CAT-CACCAACCCATTAC-3' for CLC-2 and CLC-3, respectively. The

CLC-2 forward primer is now known to be identical to mouse sequence (AF139724). The reverse primer has a G residue in place of A at position 13 of the primer sequence but is otherwise identical. PCR products were analyzed using agarose gel electrophoresis of PCR mixtures using ethidium bromide fluorescence to visualize products. PCR products were purified (QIAgel extraction kit, Qiagen, Crawley, Sussex, UK) and cloned using the TA cloning vector pCR2.1 TOPO (Invitrogen, Groningen, Netherlands). The identity of each cloned PCR product was by fluorescent di-deoxy sequencing on an ABI Prism model 377 automated sequencer. Comparison of the cloned PCR fragments to published sequence was performed using BLASTN software (www.ncbi.nlm.nih.gov) [1].

SOLUTIONS

A modified Krebs' Ringer solution was used for I_{SC} measurements of epithelial layers; its composition was (in mmol/l) NaCl, 55, mannitol 140, KCl, 5.4, CaCl₂, 2.8, MgSO₄, 1.2, KH_2PO_4 , 1.5, NaHCO_3 24, glucose 5 (pH 7.4, 37°C) gassed continuously with 95% O₂, 5% CO₂. A hypotonic solution was obtained by omitting mannitol. For patch-clamp recordings the bath solution contained (in mmol/l) NaCl, 100, KCl, 4.5, KH_2PO_4 , 1, MgCl₂, 1, CaCl₂, 2, HEPES, 10, tris(hydroxymethyl)aminomethane (TRIS), 6, glucose, 5, sucrose, 80. The pH was adjusted to 7.4 by addition of TRIS. The standard hypotonic solution was obtained by omitting sucrose. In some experiments 140 instead of 100 mmol/l NaCl (no sucrose) was used, and hypotonicity was achieved by diluting the solution with distilled H₂O. A 10-fold reduction in bath Cl⁻ (110.5 mM \rightarrow 11.05 mM) was obtained by replacement of an equivalent amount of NaCl with NaAspartate. The osmolarity of the bath solutions for patch-clamp experiments was 300 mosmol/kg H₂O and 220 mosmol/kg H₂O for the hypotonic bath solutions. Osmolarity was measured by freezing point depression (Micro-Osmometer Type 13, Roebling, Berlin, Germany). The pipette solution contained (in mmol/l): NaCl, 10, KCl, 130, MgCl₂, 2, HEPES, 10 and nystatin (100–300 $\mu\text{g}/\text{ml}$). The pH was adjusted to 7.2 by addition of TRIS. The osmolarity of the pipette solution was 270 mosmol/kg H₂O (Boese et al., 1996). Anion selectivity of conductance was determined by replacing bath NaCl with NaI or NaBr, respectively.

Perfusion of 300–500 nM Ca²⁺ into the cells cytoplasm via patch pipette (Ca²⁺ has finite permeability via the nystatin pore) was used in some experiments to activate CaCC. Appropriate amounts of CaCl and EGTA were added to the pipette solution to achieve these free Ca²⁺ concentrations.

In fast whole-cell patch-clamp experiments the bath solution contained (in mM): CsCl, 140, HEPES, 12 and TRIS, 8 (pH 7.4). Bath osmolarity was adjusted to 600 mosmol/kg H₂O by addition of sucrose. Hypotonicity was achieved by omission of 100 mM sucrose. The pipette solution contained (in mmol/l): CsCl, 140, CsOH, 10, HEPES, 20, EGTA, 1 and ATP, 2 (pH 7.2). Pipette osmolarity was adjusted to 580 mosmol/kg H₂O by addition of sucrose.

MATERIALS

The chloride channel blocker 4,4'-diisothiocyanostilbene-2,2'-disulfonic acid (DIDS [100 μM]), 5-nitro-2-(3-phenylpropylamino)benzoate (NPPB [100 μM]; TOCRIS, Bristol, UK) tamoxifen [10 μM], niflumic acid (NFA, [500 μM]) were made up as 10–100 mM stock solutions in dimethylsulfoxide (DMSO) and then diluted to give final bath concentrations. Forskolin (TOCRIS) and PDBu (Calbiochem-Novabiochem, Nottingham, UK) were made as stock solution in DMSO and used at 10–20 μM and 100 nM, respectively. DMSO at the concentrations used was without effect. Culture media and chemicals

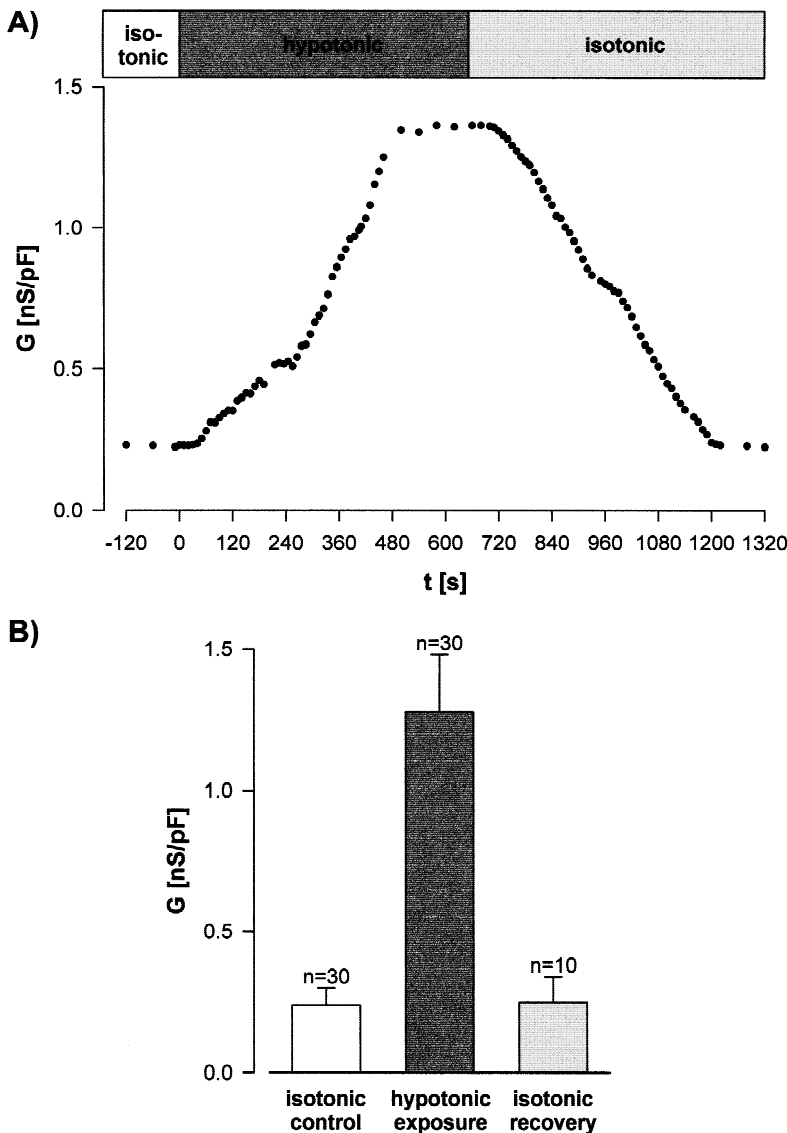


Fig. 1. (A) Reversible stimulation of whole cell conductance ($I_{Cl,swell}$) by hypotonic exposure (omission of sucrose) in mIMCD-K2 cells. (B) Summary of whole-cell conductance values normalized for cell capacitance in isotonic (control), hypotonic and after recovery (isotonic).

used were from Sigma and were of the highest purity available unless stated otherwise.

STATISTICS

Data are expressed as mean values \pm SEM for n separate epithelial layers or cells. Significance of difference between mean values was determined using ANOVA with Bonferroni-corrections for multiple comparisons applied to Student's t test (unpaired/paired data) for tests between individual data pairs (where appropriate). The level of significance was set at $P < 0.05$.

Results

BIOPHYSICAL PROPERTIES OF $I_{Cl,swell}$

A reduction in extracellular osmolarity from 300 to 220 mosm/kg H₂O (at constant ionic strength by omission of

sucrose) increases whole-cell conductance, which is reversed upon restoration of the standard bath tonicity (Fig. 1A). The slope conductance increased from 0.24 ± 0.06 nS/pF ($n = 30$) under isotonic conditions (control) to 1.28 ± 0.2 nS/pF ($n = 30$), $P < 0.001$, Fig. 1B) after reduction of bath osmolarity. Reestablishing isotonic conditions returned the conductance to 0.25 ± 0.09 nS/pF ($n = 10$ n.s. vs. controls). Activation of the conductance started 62 ± 11 sec ($n = 30$) after the change in bath osmolarity, reached steady state after 205 ± 25 sec ($n = 30$) and returned to control levels following reestablishment of isotonic conditions after 221 ± 32 sec ($n = 10$). This slow development of whole cell conductance contrasts with the expected time course of osmotic equilibration; under whole cell conditions the cellular tonicity is essentially clamped by the effective volume of the pipette solution. (Tinel et al. [36] showed that rat IMCD cells in primary culture swell to 135% of control volume

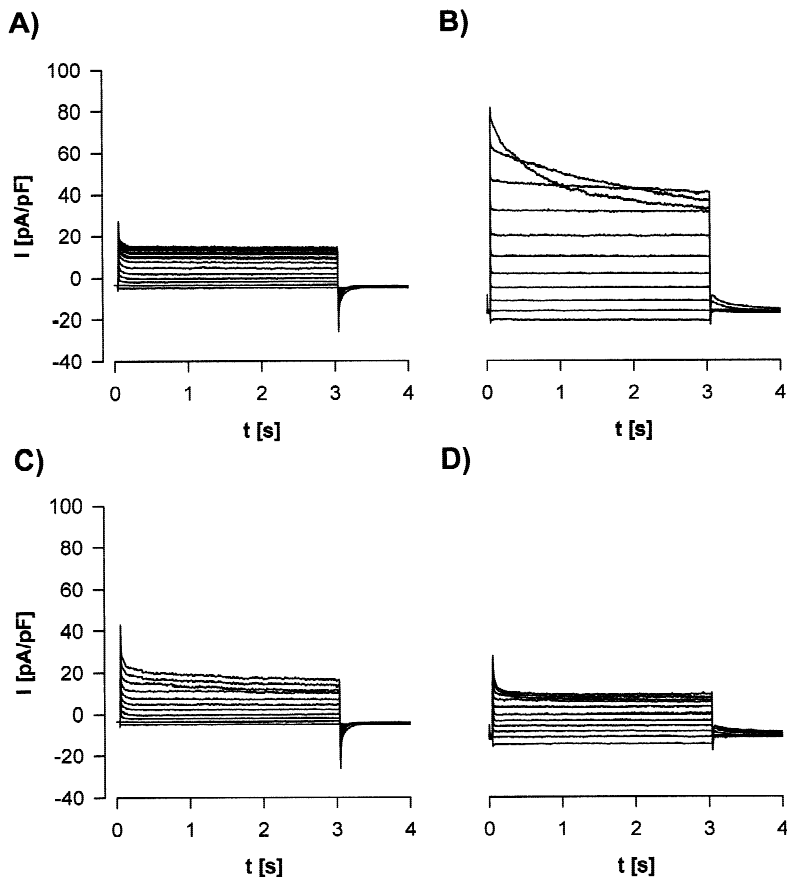


Fig. 2. Voltage-dependence of whole-cell currents. The voltage protocol used was -80 to $+120$ mV in 20 mV increments starting from a holding potential of -60 mV (see Methods). (A) Isotonic control conditions, (B) 10 min after hypotonic shock, (C) 10 min after return to isotonic conditions, (D) when bath chloride was reduced 10 -fold under hypotonic conditions.

in less than 1 min. We were also able to confirm that cell swelling occurred by direct visual observation using $\times 400$ phase contrast optics.)

A 10 -fold reduction in bath Cl^- concentration following hypotonic activation of $I_{Cl,swell}$ reduced the outward current (inward Cl^- movement at $+60$ mV) to a level not significantly different from isotonic control conditions (8.4 ± 1.5 to 8.2 ± 1.2 pA/pF, n.s., $n = 10$). But the inward current (outward Cl^- movement at -60 mV) is largely unaffected (-15.1 ± 1.0 to -14.6 ± 1.0 pA/pF, n.s., $n = 10$) (see Fig. 2A, B and D). There was a concurrent shift in the reversal potential of 34.4 ± 0.5 mV ($n = 5$). The conductance displayed an anion selectivity [P_x^-/P_{Cl^-}] of: I^- (1.4 ± 0.02 , $n = 4$) $> Br^-$ (1.1 ± 0.04 , $n = 4$) $\geq Cl^- > Asp^-$ (0.2 ± 0.01 , $n = 10$).

The current activated by cell swelling exhibited outward rectification and time and voltage dependent inactivation at positive potentials ($\geq +60/80$ mV, Fig. 2B).

INFLUENCE OF $[Ca^{2+}]_i$

Reducing the osmolarity of the bath solution (140 mM NaCl, 300 mosmol/kg H₂O) by dilution with distilled water (to 225 mosmol/kg H₂O) also activated $I_{Cl,swell}$ (Fig. 3). However, changing both ionic compositions to-

gether with bath osmolarity had additional effects on cellular conductance (compare Fig. 1A with Fig. 3). The activation of $I_{Cl,swell}$ was preceded by a brief and transient activation of an additional Cl^- conductance whose characteristics were distinct and resembled the Ca^{2+} -activated Cl^- conductance (CaCC) present in these cells [4]. Activation of CaCC has always been correlated with an increase in intracellular Ca^{2+} [4]. Comparison of the time course of the conductance increase in Fig. 3 with that seen in Fig. 1 suggests that CaCC remains active until ~ 150 sec post stimulus with bath dilution. Microspectrofluorimetry of fura-2 loaded mIMCD-K2 cells during hypotonic challenge failed, however, to detect significant change in global intracellular calcium (*unpublished observations*) suggesting that only a local change in calcium concentration close to the membrane occurs.

Cell-swelling by reducing extracellular osmolarity, but without accompanied changes in ionic composition, did not activate CaCC (Fig. 1A) suggesting that a reduction in bath Na^+ , perhaps acting via Na^+/Ca^{2+} exchange, may be involved in the transient activation of CaCC. Taken together these results indicate that changes in intracellular Ca^{2+} are not required for activation of $I_{Cl,swell}$ in mIMCD-K2 cells.

To confirm this finding, the response to hypotonic

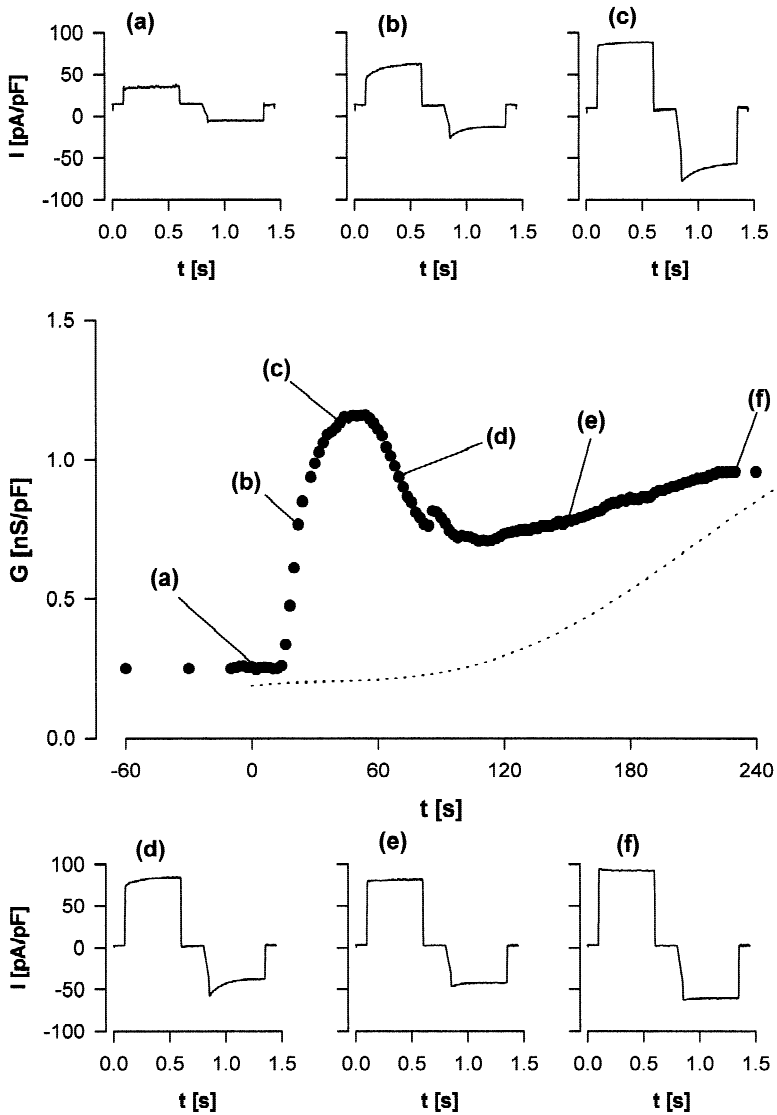


Fig. 3. Stimulation of whole-cell conductance by reduction in both bath osmolarity and ionic strength. The dashed line shows the normalized mean time course in whole cell conductance increase under purely hypotonic (Fig. 1) conditions for comparison. (a–f) Show whole-cell currents recorded with the standard protocol (pulse to +80 mV followed by a pulse to -80 mV) at the time indicated.

challenge was measured using the fast-whole cell configuration, employing both nominally Ca^{2+} -free pipette and bath solutions (see Materials and Methods). Hypotonic exposure increased membrane conductance from $0.04 \pm 0.01 \text{ nS/pF}$ to $1.0 \pm 0.2 \text{ nS/pF}$ ($n = 3$, $P < 0.001$). The activated conductance showed biophysical characteristics identical to those seen in slow whole-cell experiments (*data not shown*) and the reversal potential was $0.6 \pm 0.2 \text{ mV}$, close to the predicted Cl^- reversal potential of 0 mV in these conditions. Omission of ATP from the pipette solution in the fast whole cell configuration and incubation for at least 20 min in isotonic conditions prevented the cell-swelling dependent increase in whole cell conductance. Basal conductance changed from $0.05 \pm 0.01 \text{ nS/pF}$ under isotonic conditions to only $0.07 \pm 0.02 \text{ nS/pF}$ after a 15 min hypotonic challenge ($n = 3$, *n.s.*).

PHARMACOLOGY OF $I_{Cl,swell}$

To characterize further $I_{Cl,swell}$ present in mIMCD-K2 cells, the effect of the Cl^- channel inhibitors 5-nitro-2-(3-phenylpropylamino)benzoate (NPPB), tamoxifen, ni-flumic acid (NFA) and 4,4'-diisothiocyanostilbene-2,2'-disulfonic acid (DIDS) were tested (Fig. 4). NPPB caused the most inhibition, $91 \pm 4\%$ ($n = 5$) of the activated conductance at $100 \mu\text{M}$. Tamoxifen ($10 \mu\text{M}$) and NFA ($500 \mu\text{M}$) inhibited the swelling-activated anion conductance by $73 \pm 4\%$ ($n = 8$) and $45 \pm 2\%$ ($n = 5$), respectively. NPPB, tamoxifen and NFA inhibition of $I_{Cl,swell}$ did not display any significant voltage dependency. In contrast, DIDS ($100 \mu\text{M}$) blocked the current with a characteristic voltage dependency: $82 \pm 2\%$ at $+80 \text{ mV}$ and $47 \pm 2\%$ at -80 mV ($n = 10$, see Fig. 4a and c). The block of the hypotonic-activated current was

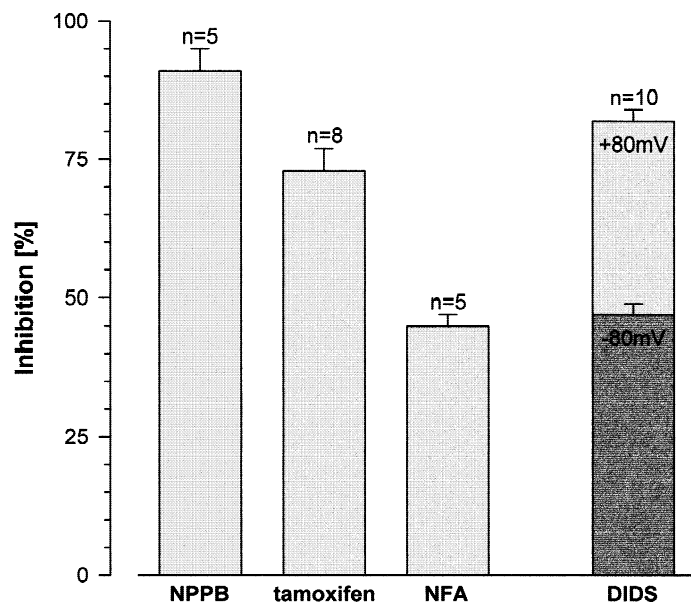
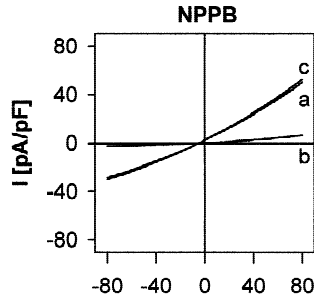
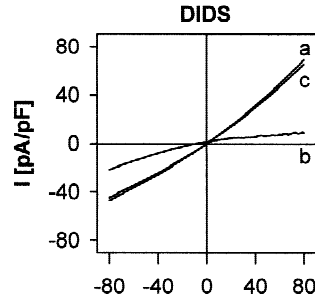
A)**B)****C)**

Fig. 4. Effect of anion channel blockers on $I_{Cl,swell}$. (A) Blockade is represented as percent (%) inhibition of the maximum values of $I_{Cl,swell}$ after hypotonic exposure. Reversal of inhibition was observed after drug withdrawal for all conditions (see B and C). Note that DIDS inhibition was voltage-dependent, both ± 80 mV mean data being represented (see C). (B and C) Voltage ramps showing the effect of NPPB and DIDS on $I_{Cl,swell}$. (a) control, (b) drug application (100 μ M), (c) washout.

completely reversible for all drugs tested (see Fig. 4b and c).

PKC REGULATION OF $I_{Cl,swell}$

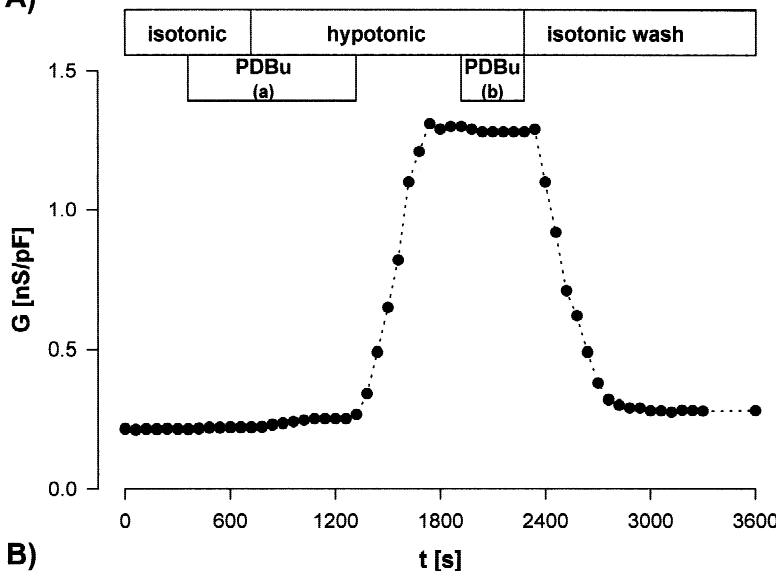
PKC activation by PDBu inhibits CLC-3 mediated Cl^- conductances and this has now been established as a key criterion for establishing the molecular identity of $I_{Cl,swell}$ (see Introduction). Accordingly we have investigated the modulatory effect of PKC by external application of PDBu (100 nM). Application of PDBu had variable effects if $I_{Cl,swell}$ was already activated. In 4 out of 20 experiments PDBu reduced the current in a voltage-independent manner to $23 \pm 3\%$ (at ± 80 mV) but had no effect on the conductance in the other 16 experiments ($101 \pm 2\%$). But as shown in Fig. 5a, if cells were exposed to PDBu before or concomitantly with hypotonic exposure, no activation of whole cell conductance was

seen (plus PDBu values were $113 \pm 32\%$, $n = 10$, n.s. vs. controls). Withdrawal of PDBu from the hypotonic bath solution resulted in the prompt activation of $I_{Cl,swell}$ but this was however refractory to subsequent PDBu inhibition (Fig. 5a).

INTERACTION OF $I_{Cl,swell}$ WITH CaCC AND CFTR Cl^- CONDUCTANCE

Besides the swelling-activated anion channel a further two Cl^- conductances, the Cystic Fibrosis Transmembrane Conductance Regulator (CFTR) Cl^- channel [40] and a Ca^{2+} activated Cl^- Conductance (CaCC) which may be related to the recently cloned CLCA1 protein [4, 17] have been identified in mIMCD-K2 cells. Both conductances are involved in transepithelial Cl^- secretion and are therefore present at the apical plasma membrane. Furthermore, we have confirmed that both con-

A)



B)

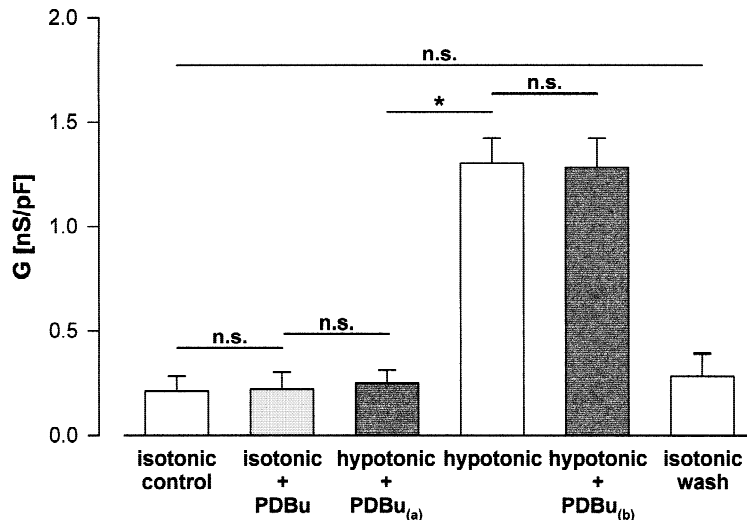


Fig. 5. Effect of PDBu on $I_{Cl,swell}$. (A) Sequential experimental data where PDBu preincubation (100 nM) abolishes the development of $I_{Cl,swell}$, removal of PDBu then allows the full development of $I_{Cl,swell}$, but this is now refractory to PDBu inhibition. Reversal of $I_{Cl,swell}$ occurs upon restoration of medium tonicity. (B) Mean data ($n = 10$).

ductances are present in a single cell [4]. Both conductances display biophysical characteristics profoundly different from $I_{Cl,swell}$. Activation of CFTR by extracellular forskolin (10 μ M) led to a linear conductance without time- or voltage-dependent kinetics (Fig. 6b). Activation of CaCC by increasing pipette $[Ca^{2+}]$ produces a strongly outwardly rectifying conductance with pronounced time-dependent current inactivation and activation at hyperpolarizing and depolarizing membrane potentials, respectively (Fig. 6a). Activation of either one of these Cl^- conductances prior to hypotonic challenging the cells had no effect on the subsequent activation of $I_{Cl,swell}$ nor on the inactivation after return to isotonic conditions (Fig. 6c and d and 7). Application of 100 nM PDBu after activation of CFTR or CaCC had no effect on these currents, but importantly, PDBu failed to prevent

activation of $I_{Cl,swell}$ after prior activation of CFTR or CaCC (Fig. 7 and compare to results in Fig. 5).

CELLULAR LOCATION

To reveal the likely cellular localization (apical or basolateral) of the swelling-activated anion conductance epithelial layers of mIMCD-K2 cells were established on permeable filters (see Methods). mIMCD-K2 epithelia layers mounted in Ussing chambers and bathed in a modified Krebs (79 mM NaCl, 140 mM mannitol) respond to apical addition of 10 μ M forskolin by a prompt stimulation of a maintained inward I_{sc} of $5.6 \pm 0.7 \mu$ A/cm 2 ($n = 6$, Fig. 8A). This is due to transepithelial Cl^- secretion mediated via apical CFTR [40] and corre-

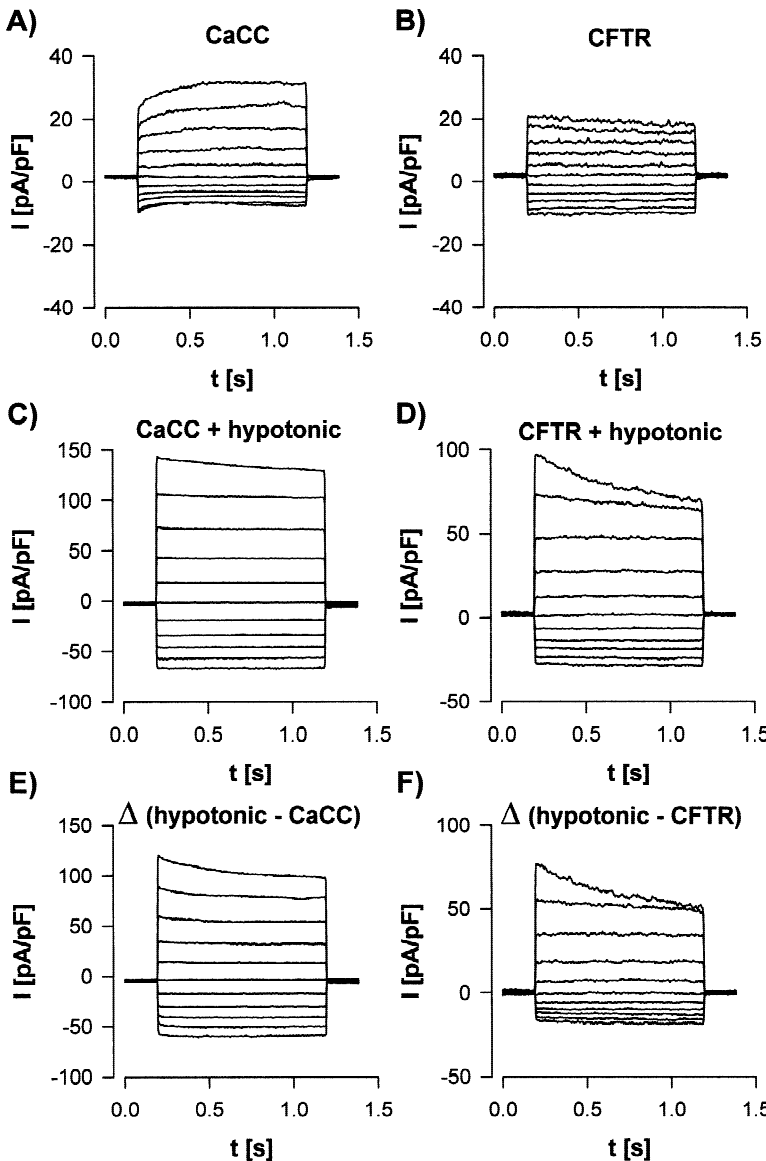


Fig. 6. Voltage-dependence of whole-cell currents after stimulation by “ Ca^{2+} -perfusion” (500 nM) “CaCC” (A) or 10 μM forskolin “CFTR” (B), alone and in combination with the hypotonic bath stimulus (C and D). (E and F) Computed difference between A/C and B/D, respectively.

lates with the increased whole-cell conductance seen with forskolin (*above*). Figure 8A shows that hypotonic exposure of the basolateral surfaces (75 mM NaCl Kreb’s) does not result in further stimulation of transepithelial inward I_{sc} . Instead it results in a prompt inhibition of the forskolin-stimulated I_{sc} to $1.0 \pm 0.4 \mu\text{A}/\text{cm}^2$, which is reversed upon restoration of basal-bathing solution tonicity ($5.2 \pm 0.4 \mu\text{A}/\text{cm}^2$). After ten minutes preincubation with 100 μM tamoxifen, the forskolin-stimulated I_{sc} was $4.40 \pm 0.41 \mu\text{A}/\text{cm}^2$ ($n = 5$, *n.s.* vs. controls minus tamoxifen), however hypotonic exposure was now virtually without effect upon transepithelial current flow, ($P < 0.001$ for tamoxifen reversal of reduction of forskolin-stimulated I_{sc} , Fig. 8B). This data thus correlates both with the reversible activation of $I_{Cl,swell}$

by bath tonicity and its inhibition by tamoxifen (Fig. 4A), and may be explained by the localization of the swelling-activated Cl^- conductance to the basolateral membrane. Activation of $I_{Cl,swell}$ will therefore control transepithelial anion secretion by decreasing the electrochemical driving force for Cl^- across the apical membrane. PDBu (100 nM) exposure during hypotonic challenge could not reverse swelling-activated inhibition of Cl^- secretion. Forskolin-activation increased I_{sc} to $4.4 \pm 0.6 \mu\text{A}/\text{cm}^2$ which was reduced to $1.1 \pm 0.4 \mu\text{A}/\text{cm}^2$ ($n = 7$, $P < 0.05$) by hypotonic treatment, but basolateral exposure to PDBu (100 nM) did not reverse this inhibition ($1.0 \pm 0.8 \mu\text{A}/\text{cm}^2$). Similarly, PDBu exposure for 10 min prior to hypotonic exposure did not effect either the forskolin-stimulated secretion ($5.2 \pm 0.5 \mu\text{A}/\text{cm}^2$, $n = 5$) nor the

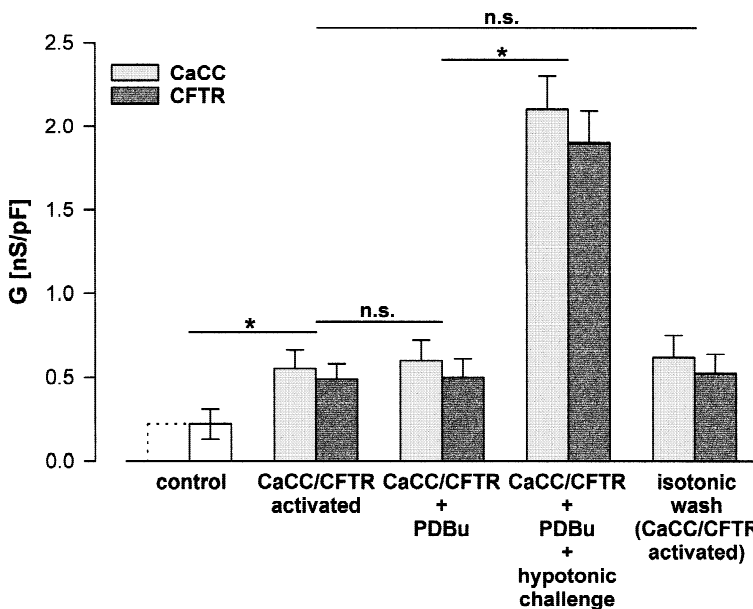


Fig. 7. Summary of sequential experiments showing the abolition of PDBu (100 nM) inhibition on $I_{Cl,swell}$ after preactivation of “CaCC” or by preactivation of “CFTR” by 10 μ M forskolin. See text for details.

hypotonic inhibition (to $1.6 \pm 0.4 \mu\text{A}/\text{cm}^2$, $n = 5$, $P < 0.01$ vs. forskolin alone, *n.s.* vs. levels in the absence of PDBu).

After continued exposure to basolateral hypotonic media there is a progressive recovery of forskolin-stimulated I_{sc} (Fig. 8A). At 6 min post exposure, inward I_{sc} recovered to $46.0 \pm 8.4\%$ of the forskolin-stimulated values after attaining a minimal value of $18.6 \pm 6.3\%$ at 2 min exposure ($n = 4$, $P < 0.05$ vs. 6 min). These data are consistent with $I_{Cl,swell}$ progressively restoring cell volume (RVD, *see also* [36]), then switching off and so relieving the observed inhibition of forskolin-stimulated I_{sc} .

CLC EXPRESSION IN MIMCD-K2 CELLS

We have utilized a RT-PCR approach to correlate the biophysical and pharmacological data to the molecular expression of both CLC-2 and CLC-3 mRNA in mIMCD-K2 cells. Using gene-specific primers (*see Materials and Methods*) to amplify reverse-transcribed mRNA, a major PCR product of 972 bp was identified in mIMCD-K2 epithelial cells (Fig. 9) consistent with mCLC-3 mRNA expression. This result cannot arise due to genomic DNA contamination since on omission of reverse transcriptase, a PCR product is not evident in mIMCD-K2 samples. Cloning and sequencing of the PCR product in both forward and reverse orientations further confirm identity to mCLC-3. We also determined if there was expression of CLC-2. A PCR product of 343 bp was identified consistent with mCLC-2 expression (Fig. 9). Alignment of mIMCD-K2 and published murine CLC-2 and 3 peptide sequence showed

only one exchange in each sequenced fragment (identity >99%). (This exchange might be due to Taq errors.)

Discussion

In this study, we have characterized $I_{Cl,swell}$ in the mouse renal epithelial cell line, mIMCD-K2. Its properties closely resemble those reported for other cell types, including glial [21], intestinal [25], and primary cultured kidney cells [7, 8, 33]. Variation in these basic properties occur mainly in the response to pharmacological agents and in the exact voltage dependence of $I_{Cl,swell}$. We conclude that mIMCD-K2 cells provide an appropriate cellular context to investigate $I_{Cl,swell}$ in renal epithelial cells.

Whereas there is general agreement concerning the basic features of the biophysical and pharmacological profile of $I_{Cl,swell}$, the molecular identity of this channel has remained controversial. Several proteins have been proposed as underlying the swelling-activated conductance but only CLC-2 and CLC-3 are now considered to be likely candidates underlying $I_{Cl,swell}$ (*see Introduction*). Our own data reported here show that CLC-2 mRNA is expressed in mIMCD-K2 cells but no biophysical signature typical of CLC-2 was noted at the plasma membrane in whole-cell patch-clamp experiments. Even after strong hyperpolarization (-100 to -150 mV) CLC-2 like currents were never seen ($n = 5$, *data not shown*). Taken together, it seems likely that CLC-2 may be expressed within endomembranes in mIMCD-K2 cells and is not trafficked to the plasma membrane even after cell swelling.

In contrast to CLC-2, CLC-3 expressed in NIH/3T3

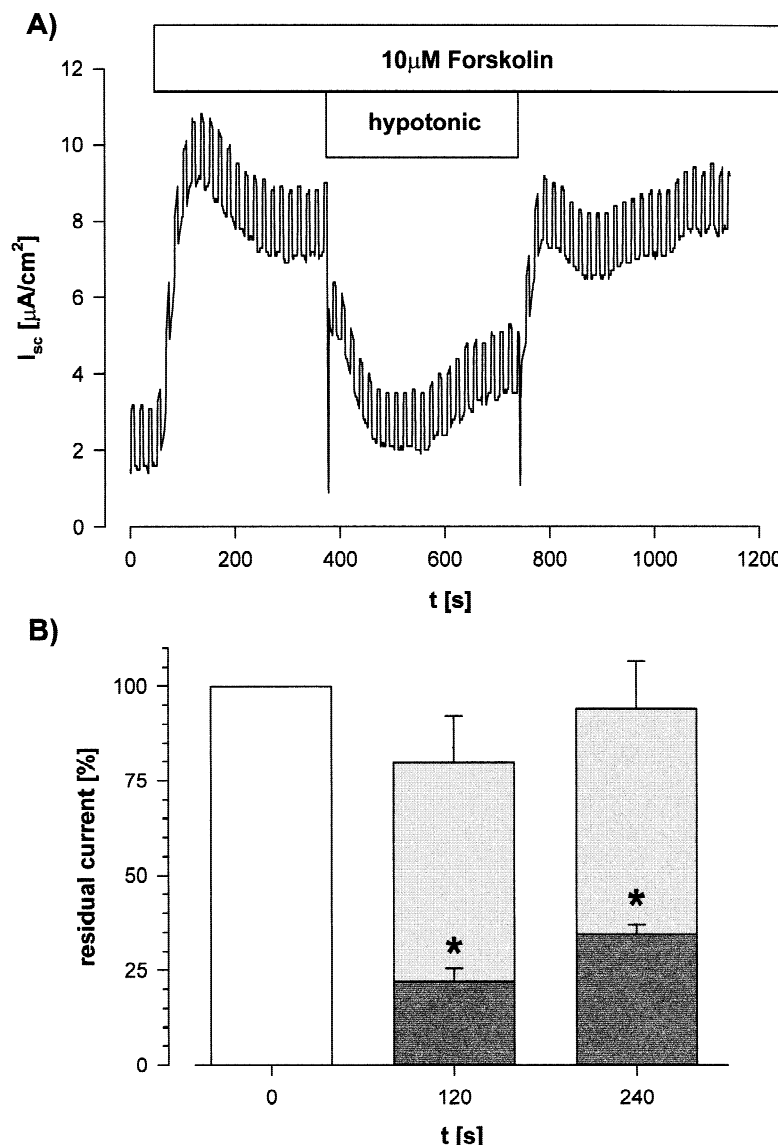


Fig. 8. Influence of hypotonic media upon forskolin ($10\text{ }\mu\text{M}$) stimulated inward I_{sc} (chloride secretion) in mIMCD-K2 epithelial layers mounted in Ussing chambers. (A) Illustrative record, including excursions of the voltage clamp by 0.5 mV to measure epithelial resistance. (B) Mean data ($n = 5$) showing hypotonic inhibition (dark grey) of I_{sc} and its reversal by $100\text{ }\mu\text{M}$ tamoxifen (light grey). For details see text.

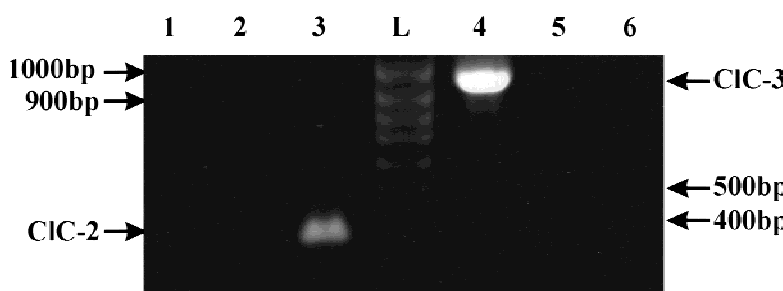


Fig. 9. Ethidium-stained agarose gel showing RT-PCR products generated with mCLC-2 and mCLC-3 gene-specific primers. Lane 1, CLC-2 RT control, Lane 2, CLC-2 PCR control, Lane 3, CLC-2, Lane 4, CLC-3, Lane 5, CLC-3 RT control, Lane 6, CLC-3 PCR control, L, size ladder.

fibroblasts produced a conductance with an anion selectivity, pharmacology and voltage dependence similar to $I_{Cl,swell}$ [13]. In native tissues, $I_{Cl,swell}$ is normally not active under isotonic conditions, but transfection with CLC-3 conferred a large Cl^- conductance even under

nonswollen, isotonic, conditions [13]. A plausible reason for this discrepancy may be the lack of an associated regulatory subunit, similar to the β unit found in voltage-gated cation channels (see e.g. [32]). An additional discrepancy resides in the regulation of $I_{Cl,swell}$ by PKC.

Heterologously expressed CLC-3 conductances are inhibited by PKC activation (mediated by phosphorylation of Ser51 of CLC-3, [14]). In native tissues there are conflicting reports on the sensitivity of $I_{Cl,swell}$ to PKC activation: In human nonpigmented ciliary cells $I_{Cl,swell}$ was inhibited by PKC activation, whereas HeLa cells $I_{Cl,swell}$ was insensitive to PKC activation (see [39]), while in pancreatic duct cells $I_{Cl,swell}$ activation was prevented by PKC inhibition [41]. Our data on mIMCD-K2 cells on the effect of PKC activation are similar to those reported for brain endothelial cells [42]. $I_{Cl,swell}$ is indeed inhibited by PKC-activation but only if PKC is stimulated prior to cell swelling. Furthermore, we have now demonstrated that a rise in intracellular Ca^{2+} or forskolin exposure, resulting in activation of CaCC or CFTR, respectively, preceding the hypotonic shock eliminates any sensitivity of $I_{Cl,swell}$ to PKC activation. How do these diverse stimuli apparently cause this common cellular response? We speculate that a change in intracellular ionic strength or chloride concentration after activation of an anion conductance may modulate the ability of PKC to affect $I_{Cl,swell}$. Pederson et al. [31] showed that variation in ionic strength and Cl^- concentration may directly regulate phosphatase activity. Specifically, amino acid-induced swelling of hepatocytes resulted in a decrease of cellular chloride, which lead to de-inhibition of glycogen synthase phosphatase. Recently, Bize et al. [3] have demonstrated that membrane-bound serine/threonine protein phosphatases (S/T-PPases) are regulated by ionic strength and/or cell size in human red blood cells. Protein phosphatases type 1 (PP1) and type 2A (PP2A) are present in these cells where their activity is elevated after exposure to hypotonic media. K-Cl cotransport is stimulated and is associated with RVD. PP1 activity is more responsive to the decrease in intracellular ionic strength while PP2A activity is differentially responsive to an increase in cell size. Further work is needed to test whether phosphatase activity may be regulated in a comparable fashion in mIMCD-K2 cells, and whether this can account for the different sensitivity of $I_{Cl,swell}$.

Duan et al. [14] showed that CLC-3 currents are blocked by an increase in intracellular Ca^{2+} (ionomycin treatment) presumably via activation of PKC. Chou et al. [11] found that at least in HT-3 cells PKC- α and extracellular Ca^{2+} regulate RVD responses and $I_{Cl,swell}$. We have previously demonstrated that an ionomycin or ATP mediated increase in intracellular Ca^{2+} activated CaCC in mIMCD-K2 cells [4]. The present data clearly show that whereas increases in intracellular Ca^{2+} may indeed activate CaCC, they do not prevent activation of $I_{Cl,swell}$ in mIMCD-K2 cells. Furthermore the time course for activation of CaCC with bath dilution is distinct from the time course for activation of $I_{Cl,swell}$. PKC- α is directly calcium sensitive and Nishino et al.

[27] showed that PKC- α activity is not affected by changes in ionic strength but by an increase in pH due to preferential association of PKC- α with the plasma membrane. These findings imply that the inhibition observed by PDBu occurs by activation of calcium independent PKC isoforms. Clearly the isoforms expressed in different cells will be cell-specific.

Further differences between $I_{Cl,swell}$ recorded in various cell types and the CLC-3 conductance relate to the extent of voltage-dependent inactivation seen at positive potentials and the sensitivity to different pharmacological agents. We clearly show that cell swelling upon bath dilution may stimulate both CaCC and $I_{Cl,swell}$ but with different time courses. With only a change in medium tonicity (omission of inert sugar) only $I_{Cl,swell}$ is stimulated. While the biophysical properties of the two conductances are distinct, coactivation of the conductances gives rise to whole cell conductances with properties that are the sum of individual conductances (Fig. 6c and d). We therefore propose that the variation in the properties of $I_{Cl,swell}$ observed between cell types depends both on the nature of volume perturbation and the complement of conductances present. Other explanations are possible e.g., that alternative splicing of a single gene that encodes the swelling-activated anion channel as it is seen in Ca^{2+} -channels [10] may give rise to divergent channel properties. It is also possible that $I_{Cl,swell}$ is mediated by a complex of more than one protein (CLC-2/CLC-3 complex?). So far there is evidence for at least one heteromeric CLC channel, a CLC-1/CLC-2 heterooligomer, which possess biophysical characteristics when expressed in *Xenopus* oocytes not seen if CLC-1 or CLC-2 mRNA is expressed singly [26]. mIMCD-K2 cells express multiple CLC family members including CLC-2, 3 and 5 (CLC-2 and 3 this study, CLC-5 *unpublished observation*). However, heterologous expression of CLC-5 in CHO cells gives rise to a weakly DIDS sensitive strongly outwardly rectifying Cl^- conductance that shows time-dependent activation rather than inactivation at positive membrane potentials (Stewart, Sayer, Gray & Simmons, *submitted*).

Finally, we have localized $I_{Cl,swell}$ to the basolateral surface of the mIMCD-K2 cell-line on the basis of cell-swelling inhibition of a concurrent transepithelial Cl^- secretion. Since intracellular osmolytes, including amino acids such as taurine, permeate via $I_{Cl,swell}$ in the IMCD [8] cellular loss will be directed to the vascular compartment rather than the tubule lumen. In addition the ability of $I_{Cl,swell}$ to effectively “short-circuit” transepithelial Cl^- secretion demonstrates an unexpected regulatory role for $I_{Cl,swell}$ in secretory epithelia.

In conclusion, the characteristics of $I_{Cl,swell}$ in renal mIMCD-K2 are broadly consistent with that expected for CLC-3 protein expression. The slow activation of $I_{Cl,swell}$ relative to volume change suggests that the

mIMCD-K2 cell line may be an ideal model in which to investigate the mechanism by which cell swelling (via phosphorylation, or endomembrane traffic) may stimulate $I_{Cl,swell}$ at the basolateral plasma membrane.

The work was supported by a grant from the Wellcome Trust to MAG/NLS. MG was supported by the BHF.

References

- Altschul, S.F., Madden, T.L., Schaffer, A.A., Zhang, J.Z.Z., Miller, W., Lipman, D.J. 1997. Gapped BLAST and PSI-BLAST: a new generation of protein database search programs. *Nuc. Acid Res.* **25**:3389–3402
- Beck, F.X., Dröge, A., Thurau, K. 1988. Cellular osmoregulation in renal medulla. *Renal Physiol. Biochem.* **11**:174–186
- Bize, I., Güvenç, B., Robb, A., Buchbinder, G., Brugnara, C. 1999. Serine/threonine protein phosphatases and regulation of K-Cl co-transport in human erythrocytes. *Am. J. Physiol.* **277**:C926–C936
- Boese, S.H., Glanville, M., Aziz, O., Gray, M.A., Simmons, N.L. 2000. Ca^{2+} and cAMP-activated Cl^- conductances mediate Cl^- secretion in a mouse renal inner medullary collecting duct cell line. *J. Physiol.* **523**:325–338
- Boese, S.H., Glanville, M., Gray, M.A., Simmons, N.L. 1999. Characterization of a swelling-activated Cl^- conductance in mouse renal inner medullary collecting duct cells (mIMCD-K2). *J. Physiol.* **517P**:66P
- Boese, S.H., Glanville, M., Simmons, N.L., Gray, M.A. 1999. The swelling-activated chloride conductance in mIMCD-K2 cells is associated with multiple CLC expression *FASEB J.* **5**:A712
- Boese, S.H., Kinne, R.K.H., Wehner, F. 1996. Single-channel properties of swelling-activated anion conductance in rat inner medullary collecting duct cells. *Am. J. Physiol.* **271**:F1224–F1233
- Boese, S.H., Wehner, F., Kinne, R.K.H. 1996. Taurine permeation through swelling-activated anion conductance in rat IMCD cells in primary culture. *Am. J. Physiol.* **271**:F498–F507
- Bond, T.D., Ambikapathy, S., Mohammad, S., Valverde, M.A. 1999. Osmosensitive Cl^- currents and their relevance to regulatory volume decrease in human intestinal T-84 cells: outwardly vs. inwardly rectifying currents. *J. Physiol.* **511**:45–54
- Bourinet, E., Soong, T.W., Slaymaker, S., Mathews, E., Monteli, A., Zamponi, G.W., Snutch, T.P. 1999. Splicing of alpha 1a subunit generates phenotypic variants of P- and T-type calcium channels. *Nat. Neurosci.* **2**:407–415
- Chou, C.Y., Shen, M.R., Hsu, K.S., Huang, H.Y., Lin, H.C. 1998. Involvement of PKC-alpha in regulatory volume decrease responses and activation of volume-sensitive chloride channels in human cervical cancer HT-3 cells. *J. Physiol.* **512**:435–448
- Clapham, D.E. 1998. The list of potential volume-sensitive chloride currents continues to swell (and shrink). *J. Gen. Physiol.* **111**:623–624
- Duan, D., Winter, C., Cowley, S., Hume, J.R., Horowitz, B. 1997. Molecular identification of a volume-regulated chloride channel. *Nature* **390**:417–421
- Duan, D., Cowley, S., Horowitz, B., Hume, J.R. 1999. A serine residue in CIC-3 links phosphorylation-dephosphorylation to chloride channel regulation by cell volume. *J. Gen. Physiol.* **113**:57–70
- Emma, F., Breton, S., Morrison, R., Wright, S., Strange, K. 1998. Effect of cell swelling on membrane and cytoplasmic distribution of pI(Cln). *Am. J. Physiol.* **274**:C1545–C1551
- Emma, F., SanchezOlea, R., Strange, K. 1998. Characterization of pI(Cln) binding proteins: identification of p17 and assessment of the role of acidic domains in mediating protein-protein interactions. *Biochem. Biophys. Acta* **1404**:321–328
- Gruber, A.D., Elble, R.C., Ji, H.L., Schreur, K.D., Fuller, C.M., Pauli, B.U. 1998. Genomic cloning, molecular characterization, and functional analysis of human CLCA1, the first human member of the family of Ca^{2+} -activated Cl^- channel proteins. *Genomics* **54**:200–214
- Gründer, S., Thiemann, A., Pusch, M., Jentsch, T.J. 1992. Regions involved in the opening of C1C-2 chloride channel by voltage and cell volume. *Nature* **360**:759–762
- Hamill, O.P., Marty, A., Neher, E., Sakmann, B., Sigworth, F.J. 1981. Improved patch-clamp techniques for high-resolution current recording from cells and cell-free membrane patches. *Pflügers Arch.* **391**:85–100
- Hoffmann, E.K., Dunham, P.B. 1995. Membrane mechanisms and intracellular signaling in cell volume regulation. *Int. Review Cyto.* **161**:173–262
- Jackson, P.S., Strange, K. 1993. Volume-sensitive anion channels mediate swelling-activated inositol and taurine efflux. *Am. J. Physiol.* **265**:C1489–C1500
- Kawasaki, M., Uchida, S., Monkawa, T., Miyawaki, A., Mokshiba, K., Marumo, F., Sasaki, S. 1994. Cloning and expression of a protein kinase C-regulated chloride channel abundantly expressed in rat brain neuronal cells. *Neuron* **12**:597–604
- Kinne, R.K.H., Boese, S.H., Kinnesaffran, E., Ruhfus, B., Tinel, H., Wehner, F. 1996. Osmoregulation in the Renal Papilla — Membranes, Messengers and Molecules. *Kidney Int.* **49**:1686–1689
- Kizer, N.L., Lewis, B., Stanton, B.A. 1995. Electrogenic sodium absorption and chloride secretion by an inner medullary collecting duct cell line (mIMCD-K2). *Am. J. Physiol.* **268**:F347–F355
- Kubo, M., Okada, Y. 1992. Volume-regulatory Cl^- channel currents in cultured human epithelial cells. *J. Physiol.* **456**:351–371
- Lorenz, L., Pusch, M., Jentsch, T.J. 1996. Heteromultimeric CLC chloride channels with novel properties. *Proc. Nat. Acad. Sci. USA* **93**:13362–13366
- Nishino, N., Sugimoto, I., Hashimoto, E. 1998. Possible role of alteration in pH, but not in ionic strength, in the modulation of Ca^{2+} -dependent and diacylglycerol-induced association of protein kinase C-alpha with plasma membrane. *Biochem. Mol. Biol. Int.* **46**:725–731
- Obermüller, N., Gretz, N., Kriz, W., Reilly, R.F., Witzgall, R. 1998. The swelling-activated chloride channel CIC-2, the chloride channel CIC-3, and CIC-5, a chloride channel mutated in kidney stone disease, are expressed in distinct subpopulations of renal epithelial cells. *J. Clin. Invest.* **101**:635–642
- Okada, Y. 1997. Volume expansion-sensing outward-rectifier Cl^- channel: Fresh start to the molecular identity and volume sensor. *Am. J. Physiol.* **273**:C755–C789
- Paulmichl, M., Li, Y., Wickman, K., Ackerman, M., Peralta, E., Clapham, D. 1992. New mammalian chloride channel identified by expression cloning. *Nature* **356**:238–241
- Pederson, B.A., Nordlie, M.A., Foster, J.D., Nordlie, R.C. 1998. Effects of ionic strength and chloride ion on activities of the glucose-6-phosphatase system: Regulation of the biosynthetic activity of glucose-6-phosphatase by chloride ion inhibition/deinhibition. *Arch. Biochem. Biophys.* **353**:141–151
- Rettig, J., Heinemann, S.H., Wunder, F., Lorra, C., Parcej, D.N., Dolly, J.O., Pongs, O. 1994. Inactivation properties of voltage-gated K^+ channels altered by presents of beta-subunit. *Nature* **369**:289–294
- Sauer, H., Kinne, R.K.H., Wehner, F. 1995. Activation of a Cl^- -conductive pathway in primary cultures of rat inner medullar col-

lecting duct (IMCD) cells under hypotonic stress. *Biochem. Biophys. Acta* **1239**:99–102

34. Strange, K., Emma, F., Jackson, P.S. 1996. Cellular and molecular physiology of volume-sensitive anion channels. *Am. J. Physiol.* **339**:C711–C730

35. Strange, K. 1998. Molecular identity of the outwardly rectifying, swelling-activated anion channel: Time to reevaluate PI_{Chn} . *J. Gen. Physiol.* **111**:617–622

36. Tinel, H., Wehner, F., Sauer, H. 1994. Intracellular Ca^{2+} release and Ca^{2+} influx during regulatory volume decrease in IMCD cells. *Am. J. Physiol.* **267**:F130–F138

37. Valverde, M.A., Diaz, M., Sepulveda, F.V., Gill, D.R., Hyde, S.C., Higgins, C.F. 1992. Volume-regulated chloride channels associated with the human multidrug-resistance P-glycoprotein. *Nature* **355**:830–833

38. Valverde, M.A., Bond, T.D., Hardy, S.P., Taylor, J.C., Higgins, C.F., Altamirano, J., Alvarez-Leefmans, F.J. 1996. The multidrug resistance P-glycoprotein modulates cell regulatory volume decrease. *EMBO J.* **15**:4460–4468

39. Valverde, M.A. 1999. CLC channels: leaving the dark ages on the verge of a new millennium. *Curr. Opin. Cell Biol.* **11**:509–516

40. Vandorpe, D., Kizer, N., Ciampolillo, F., Moyer, B., Karlson, K., Guggino, W.B., Stanton, B.A. 1995. CFTR mediates electrogenic chloride secretion in mouse inner medullary collecting duct (mIMCD-K2) cells. *Am. J. Physiol.* **269**:C683–C689

41. Verdon, B., Winpenny, J.P., Whitfield, K.J., Argent, B.E., Gray, M.A. 1995. Volume-activated chloride currents in pancreatic duct cells. *J. Membrane Biol.* **147**:173–183

42. Von Weikersthal, S.F., Margery, A.B., Hladky, S.B. 1999. Functional and molecular characterization of a volume-sensitive chloride current in rat brain endothelial cells. *J. Physiol.* **516.1**:75–84

43. Xiong, H., Li, C., Garami, E., Wang, Y., Ramjesingh, M., Galley, K., Bear, C.E. 1999. CLC-2 activation modulates regulatory volume decrease. *J. Membrane Biol.* **167**:215–221

44. Yamazaki, J., Duan, D., Janiak, R., Kuenzli, K., Horowitz, B., Hume, J.R. 1998. Functional and molecular expression of volume-regulated chloride channels in canine vascular smooth muscle cells. *J. Physiol.* **507**:729–736